Send Orders for Reprints to reprints@benthamscience.ae

Current Physical Chemistry, 2015, *5*, 5-20

Liesegang Phenomena: Spontaneous Pattern Formation Engineered by Chemical Reactions

Hideki Nabika*

Department of Material and Biological Chemistry, Faculty of Science, Yamagata University, 1-4-12 Kojirakawa, Yamagata 990-8560, Japan

Hideki Nabika

Abstract: Numerous self-organized spatiotemporal patterns are seen in Nature, many of which are controlled *via* minute balances between the reactions and diffusion of the constituents in each system. The Liesegang phenomenon is one of the major mechanisms that yield static self-organized patterns in Nature, *e.g.*, the beautiful patterns of agates. Since the discovery of the Liesegang phenomenon in chemistry, many researchers have attempted to identify the inherent mechanism to enable the engineering of desired patterns by chemical reactions. In this review, we briefly discuss the theoretical background of Liesegang phenomena, which can be used to quantitatively explain the experimental results in a number of Liesegang systems. Some recent developments in the controlled construction of Liesegang patterns are then reviewed.

Keywords: Liesegang, micropattern, nanoparticle, spatiotemporal homogeneity, spatiotemporal patterns, reaction-diffusion.

1. INTRODUCTION

High-school chemistry textbooks represent many chemical reactions by the most basic one-directional equation, *i.e.*, A + B → C + D. This equation states that the constituents A and B react over time and are converted to the reaction products C and D. This type of reaction will stop after a finite time. Later in the textbook, we would find a chapter describing chemical equilibrium, characterized by the equation A + B ⇌ C + D. At the equilibrium state, the rates of the forward and backward reactions are equal, and there is no overall net reaction. If one of these chemical reactions is induced in a glass beaker, the reaction will proceed homogeneously until its equilibrium state is reached; the chemical composition at equilibrium is independent of time and space (*t*, and *x*, *y*, and *z* coordinates). You will occasionally see more complicated chemical reactions in specialized textbooks, but most reactions are one-directional or equilibrium reactions.

*Address correspondence to these authors at the Department of Material and Biological Chemistry, Faculty of Science, Yamagata University, 1-4-12 Kojirakawa, Yamagata 990-8560, Japan; Tel/Fax: +81-23-628-4589; E-mail: nabika@sci.kj.yamagata-u.ac.jp

However, in Nature, a number of reactions occur that do not reach any state with spatiotemporal homogeneity. The formation of a non-homogeneous spatiotemporal pattern is a universal phenomenon and can be observed widely in chemical, biological, and geochemical systems. These patterns are developed without external direction; they appear spontaneously when the reactions and diffusion rates of the requisite constituents are balanced. One of the most familiar and impressive examples is the body surface of a zebra. Its black and white striped pattern remains throughout its life, and never reaches a spatially homogeneous gray color. A similar phenomenon is also found in precious stones. Agate, which is characterized by a bright striped pattern, attracts the attention of those interested in jewels or non-equilibrium chemistry. Our life is also governed by many spatiotemporally pattered rhythms. We usually wake up in the morning and go to bed at night; the next day will start the next morning. This 24 h cycle is governed not only by the Earth's rotation but also by physiological phenomena known as circadian rhythms. The circadian rhythm can "reset" physiological phenomena every 24 h in a regular life.

1877-9476/15 $58.00+.00

These spatiotemporally repeating phenomena are stabilized by the interplay between reactions and the diffusion of constituents under non-equilibrium conditions; therefore, these systems are called reaction-diffusion systems. Unlike one-directional or equilibrium reactions, which are described only by reaction terms, the behavior in a reaction-diffusion system is described by combing reaction and diffusion terms, as follows:

$$\frac{\partial c}{\partial t} = R(c) + D\nabla^2 c$$

where, c, t, R, and D are the concentration of a component, time, reaction equation, and diffusion coefficient of the component, respectively. Model reactions of spatiotemporally repeating phenomena in Nature can be achieved in the laboratory using a beaker and various chemical reagents. One of the best-known reactions is the Belousov-Zhabotinsky (BZ) reaction, which was discovered by Belousov and rediscovered by Zhabotinsky. Belousov found that a reaction solution containing bromate and citric acid in the presence of cerium(IV) sulfate exhibited a periodic change in color, and the ratio of the concentrations of cerium(IV) and cerium(III) ions in the solution oscillated. When the BZ reaction solution is poured into a petri dish, concentric or spiral waves develop. These spatiotemporal periodic oscillations can be used as a model system to understand spontaneous spatiotemporal oscillations in Nature. However, it is not reasonable to expect the dynamic BZ reaction to result in the formation of static patterns such as the black/white pattern of a zebra.

In addition to the dynamic oscillating patterns that can be modeled by the BZ reaction, there are many static spatial patterns without short-term temporal changes in Nature, as briefly mentioned previously (Fig. **1**), [1, 2]. Two of the main origins of static spatial pattern formation are known as the Turing and Liesegang phenomena. The former is known as the origin of the black/white pattern of a zebra, which arises from a spontaneous symmetry-breaking process under non-equilibrium condition and a competition between self-activation by a slow-diffusing activator and inhibition by a faster diffusing factor. A famous observation of temporal change in the stripe patterns of marine angelfish and its comparison with a simulation based on a Turing system clearly demonstrated that a Turing-type reaction-diffusion wave is a viable mechanism for stripe patterns in nature [3]. As in zebras and angelfish, the Turing pattern has been widely applied to explain spontaneously forming and spatially repetitive patterns in Nature.

The latter Liesegang reaction was discovered by the German chemist R.E. Liesegang. Several chemical systems that produce Liesegang patterns in their equilibrium states have been reported, most of which yield Liesegang patterns by salt-precipitation reactions between cations and anions. Several excellent works on Liesegang systems were seen in the 1980s [4-6]. Precipitation occurs not homogeneously but periodically in space causing spatial patterns with no short-term temporal changes to be formed, similar to the black/white pattern on a zebra. The reason that most investigations of Liesegang patterns use salt-precipitation reactions originates in its mechanistic

Fig. (1). Static patterns seen in nature. (left) Liesegang rings in an apocrine hidrocystoma. Reprinted with permission from Ref. [1], Copyright 2010, John Wiley and Sons. (middle) Baló's concentric sclerosis [2]. (right) Snapshot of zebra.

limitations. In order to yield Liesegang patterns, we have to design a reaction system that involves at least one concentration threshold. One chemical reaction that has a concentration threshold is the salt-precipitation reaction, in which the reaction proceeds only when the ionic product exceeds the solubility product. Extensive investigations of Liesegang systems have therefore been limited to salts such as hydroxides [7-16], chromates [17-22], dichromates [23-29], phosphates [30-33], carbonates [34], iodides [35-39], oxalates [40], and oxinates [41].

In this review, we briefly introduce the general theoretical background and some experimental trends that show the diversity and controllability of Liesegang pattern formation.

2. THEORETICAL BACKGROUND

2.1. General

The development of a general theoretical model that can reproduce a large number of Liesegang phenomena in Nature and artificial systems is a major challenge. Liesegang phenomena exhibit many interesting and sometimes mysterious features; therefore, it is too difficult to generalize and develop a unified theory. This is why there are several representative models, each of which can reproduce a particular feature. Before proceeding to these representative models, we briefly discuss some important points that have some generality in quantitatively explaining the experimental results in a number of Liesegang systems.

(1) Spacing Law

It has been shown experimentally in Liesegang systems that the interband distance increases with increasing separation from the interface between the inner and outer electrolytes. This characteristic of spatially ordered Liesegang bands is known as the spacing law, and is described as:

$$\frac{x_{n+1}}{x_n} = 1 + p$$

where p and x_n are the spacing coefficient and distance of the nth ring from the interface, respectively. Usually, the spacing coefficient p is positive, which corresponds to the experimental observation that the interband distance ($x_{n+1} - x_n$) becomes larger as n increases. Several experimental systems, with various p values, follow the spacing law. The magnitude of p is highly dependent on the experimental conditions. In the case of $Co(OH)_2$ Liesegang systems, p increases from 0.22 to 0.56 when the outer electrolyte (Co^{2+}) concentration is increased from 0.1 M to 0.5 M [13]. The magnitude of p can also be controlled by an external electric field; p increases with increasing applied electric field [42, 43]. A number of experiments have shown that p depends strongly on the initial electrolyte concentration, as described by the Matalon−Packter law:

$$p = f(b_0) + \frac{g(b_0)}{a_0}$$

where a_0 and b_0 are the outer and inner electrolyte concentrations, respectively.

In contrast to the consecutive increases in the interband distance ($x_{n+1} - x_n$) with increasing n, the opposite behavior, *i.e.*, consecutive decreases in the interband distance, is observed in some systems. This unique behavior is called "revert spacing". Contact between an agar gel containing the inner electrolyte $Pb(NO_3)_2$ and a solution of the outer electrolyte K_2CrO_4 results in bands of precipitated $PbCrO_4$ with decreasing interband spacing [22]. Under a wide range of experimental conditions in terms of the gel, and inner and outer electrolyte concentrations, the $PbCrO_4$ precipitate has revert spacing.

(2) Time Law

In addition to the spacing law, which regulates the spatial dynamics of band formation, Liesegang phenomena also follow a time law, which regulates temporal dynamics. The ratio (q) between x_n and the square root of the time elapsed until the nth band appears, t_n, is constant.

$$\frac{x_n}{\sqrt{t_n}} = q$$

Although reasonably satisfactory experimental results for the time law have been reported in some cases [14, 44], significant deviations also occasionally appear when the interface between the inner and outer electrolytes is not linear [28].

Generally, the time law is satisfied when the Liesegang bands are formed by planar reaction fronts. When the interface is circular, deviations from the linear relationship between x_n and the square root of t_n are observed. The deviation becomes larger with decreasing diameter of the circular interface, *i.e.*, increasing curvature of the interface.

(3) Width Law

The width law describes a common morphological feature of Liesegang bands. Each band appears at position x_n at time t_n with a characteristic width (w_n). In many cases, the band becomes broader with increasing n; therefore, w_n increases with increasing distance from the interface between the inner and outer electrolytes. The relationship between w_n and x_n can be written as a power law:

$$w_n \sim x_n^{\alpha}$$

with $\alpha > 0$. Unlike the cases for the spacing and time laws, precise experimental measurements of w_n are difficult without well-developed image-analyzing techniques. The error in w_n can therefore be large, which occasionally makes it difficult to include w_n in quantitative analyses.

2.2. Major Theoretical Models

Theoretical models describing Liesegang phenomena are mainly categorized into two types: pre-nucleation [45-47] and post-nucleation models [48-51]. In the former models, the nucleation and precipitation proceed in the same space. The nucleation depletes the surrounding constituent electrolyte below the level of some threshold for nucleation, resulting in the appearance of region-selective nucleation. In this region, precipitation follows the nucleation. The latter models do not require that the nucleation and precipitation occur in the same space, and instead region-selective precipitation occurs in the medium with homogeneously distributed nuclei.

In both pre- and post-nucleation models, it is important to determine how atoms, ions, and molecules nucleate and precipitate as solid particles in a diffusive medium. It is a prerequisite that nucleation occurs only when the free energy change for nucleation (ΔG_{nucl}) is negative, and two factors that determine ΔG_{nucl} have to be considered. One is the gain in energy that results from formation of a solid nucleus, and the other is the loss in energy owing to the formation of an interface between the medium and the solid nucleus. The total energy balance for a spherical nucleus of radius r can be written as:

$$\Delta G_{\mathrm{nucl}} = -\frac{4}{3}\pi r^3 \Lambda + 4\pi r^2 \Gamma$$

where Λ and Γ are the transition energy from the initial constituents to the solid nuclei and the surface energy per unit area, respectively. ΔG_{nucl} is positive near $r = 0$ and increases with increasing r until $\mathrm{d}\Delta G_{\mathrm{nucl}}/\mathrm{d}r = 0$ at the critical radius, r_c. For $r > r_c$, ΔG_{nucl} decreases with increasing r and becomes negative when nucleation occurs. Therefore, nucleation can occur under supersatur-ation conditions, which compensate for the loss in the interface formation energy through the gain of sufficient transition energy to fulfill $\Delta G_{\mathrm{nucl}} < 0$. It is therefore common to consider a supersaturation state for inducing Liesegang phenomena, irrespective of the model used.

2.2.1. Supersaturation Model

The first developed model was based on simple supersaturation of an ionic product [52]. The chemical process assumed in this model is A + B → P, in which oppositely charged ions, A and B, produce precipitate P [45, 46]. Unlike the other models described below, no intermediate state is involved in this model. As mentioned previously, nucleation can occur above a critical ion concentration. Precipitate P is therefore formed when the ionic product of A and B (ab) exceeds the critical value (K_1). Once precipitates form, they grow by consuming the surrounding A and B. This occurs because the energy required for A and B to form new nuclei is much higher than that needed for consumption by and growth of preformed nuclei. Precipitate growth proceeds until the local ion concentration is much less than the critical concentration. Large amounts of A and B are consumed in the initial precipitation area; therefore, an area far from the initial precipitation area becomes the

region with the highest *ab* value. A precipitate again forms when *ab* exceeds the critical value. By repeating these processes, intermittent precipitation bands (alternating precipitation and depletion regions) appear as Liesegang bands.

The differential dynamic equations for the supersaturation model are:

$$\frac{\partial a}{\partial t} = D_a \nabla^2 a - k_1 \theta(ab - K_1) - k_2 abp$$

$$\frac{\partial b}{\partial t} = D_b \nabla^2 b - k_1 \theta(ab - K_1) - k_2 abp$$

$$\frac{\partial p}{\partial t} = k_1 \theta(ab - K_1) + k_2 abp$$

where D_a and D_b are the diffusion coefficients of A and B, respectively. The rate constants for precipitation and growth are denoted by k_1 and k_2, respectively. $\theta(ab - K_1)$ is the step function such that $\theta(ab - K_1) = 1$ when $ab - K_1 \quad 0$, otherwise $\theta(ab - K_1) = 0$. This function states that the precipitation reaction A + B → P proceeds only when the ionic product *ab* exceeds the critical value K_1. The last term on the right-hand side of these equations represents the formation of P *via* aggregation on the preformed precipitate at concentration *p*.

2.2.2. Nucleation and Growth Model

The supersaturation model assumes that A and B directly form a precipitate P when their concentrations exceed a critical value. Next, we consider the case where an intermediate species C is formed before precipitation, *i.e.*, A + B → C → P. In this system, A and B react to give the intermediate C, which also diffuses in the medium. The intermediate species C could be a molecule AB or a sol consisting of A and B. Similar to the supersaturation model, the formation of intermediate C proceeds only when the ionic product *ab* exceeds the critical value, K_1. Accumulation of C finally induces the nucleation reaction C → P above a critical concentration, K_2. The nucleated P acts as a seed for further growth by consuming nearby C. This model therefore has two critical concentration parameters, which is a significant difference from the supersaturation model. The differential dynamic equations for this model are:

$$\frac{\partial a}{\partial t} = D_a \nabla^2 a - k_1 \theta(ab - K_1)$$

$$\frac{\partial b}{\partial t} = D_b \nabla^2 b - k_1 \theta(ab - K_1)$$

$$\frac{\partial c}{\partial t} = D_c \nabla^2 c + k_1 \theta(ab - K_1) - k_2 \theta(c - K_2) - k_3 cp$$

$$\frac{\partial p}{\partial t} = k_2 \theta(c - K_2) + k_3 cp$$

It should be noted again that this model has two concentration thresholds and the equations have two-step functions. Several experimental observations have been discussed based on this model [24, 27, 53].

2.2.3. Sol-Coagulation Model

In the nucleation and growth model, the intermediate species C nucleates and forms P when the concentration condition $c > K_2$ is satisfied, and the nucleated P grows by consuming nearby C. However, some charged nuclei cannot approach the preformed P, because of strong electrostatic repulsion. The DLVO theory states that an electrostatic interaction is strongly shielded by the presence of a sufficient amount of ions between two interacting charged objects-in the present case, two interacting sols, preformed nuclei and C. Precipitate growth therefore occurs only in the region where the electrolyte concentration exceeds some critical value, which is called the critical coagulation concentration (K'). The reaction medium initially contains a certain amount of inner electrolyte; therefore, the conditions under which K' is exceeded usually depend on the local concentration of the outer electrolyte. The differential dynamic equations for this sol-coagulation model [54, 55] are described as follows:

$$\frac{\partial a}{\partial t} = D_a \nabla^2 a - k_1 ab$$

$$\frac{\partial b}{\partial t} = D_b \nabla^2 b - k_1 ab$$

$$\frac{\partial c}{\partial t} = D_c \nabla^2 c + k_1 ab - k_2 \theta (c - K') - k_3 cp$$

$$\frac{\partial p}{\partial t} = k_2 \theta (c - K') + k_3 cp$$

This model has also given important insights into several experimental observations [7, 21, 23, 36].

2.2.4. Competitive Particle Growth Model

The competitive particle growth model [48] is a post-nucleation model based on the competitive particle growth of large and small particles in the same domain. Because of differences in the surface tension and solubility of large and small particles, large particles grow at the expense of small ones. Simply speaking, this model describes the result of Ostwald ripening effects after precipitation. When starting with a space with homogeneously distributed precipitates, a local fluctuation can induce a spatiotemporal pattern. Namely, a local fluctuation could promote the dissolution of a small precipitate, allowing the surrounding large precipitate to grow further using the released material. Finally, the smaller particle completely dissolves, leaving a void in the middle of the precipitate. The spatial repetition of voids and large precipitates gives a number of periodic precipitation phenomena.

2.2.5. Phase Separation Scenario

The phase separation scenario [51, 56] is also categorized as a post-nucleation model, in which the phase separation of a homogeneously nucleated intermediate induces low- and high-concentrations of precipitate, as described by the Cahn-Hillard equation. The chemical process assumed in this model is A + B → C with rate constant *k*. The differential dynamic equations for each component can be described as:

$$\frac{\partial a}{\partial t} = D_a \Delta a - kab$$

$$\frac{\partial b}{\partial t} = D_b \Delta b - kab$$

$$\frac{\partial m}{\partial t} = -\lambda \Delta (m - m^3 + \sigma \Delta m) + kab + \eta_c$$

where *m* is the appropriately scaled concentration of C. The parameters λ, σ, and η_n are the rescaled kinetic coefficient, surface tension, and conserved noise, respectively. During the precipitation process, C segregates into low (*m* = -1) and high (*m* = 1) concentration states according to spinodal decomposition. This model has been applied to many experimental systems, including $CuCrO_4$ [57], $Al(OH)_3$ [12, 58], and $Ag_2Cr_2O_7$ [23].

3. SOME TRENDS IN RECENT LIESEGANG CHEMISTRY

Because Liesegang chemistry has a long history, and much research has been conducted since its discovery in 1896, it is not possible to cover all the topics studied so far. Here, we present some selected topics that have been discussed or developed in order to construct diverse Liesegang patterns in a controllable manner.

3.1. Material Diversity

As we have seen above, Liesegang patterns can be formed by depositing inorganic salt precipitates such as hydroxides [7-16], chromates [17-22], dichromates [23-29], phosphates [30-33], carbonates [34], iodides [35-39], oxalates [40], and oxinates [41]. The formation of non-salt Liesegang patterns is a great challenge, which could offer novel chemical models for pattern formation in Nature and novel materials with intriguing structural and functional properties. Recent studies have reported the formation of such Liesegang patterns by metal nanoparticles formed *via* chemical reduction of metal ions with an appropriate reducing agent [59].

Ag^+ is a typical ion that can form precipitates with an appropriate anion in a gel matrix. For example, when an agarose gel containing Ag^+ ions is placed in a gelatin matrix doped with $Cr_2O_7^{2-}$, Ag^+ ions spontaneously diffuse into the gelatin matrix (Fig. **2**, top panel) [23]. $Ag_2Cr_2O_7$ then precipitates and forms periodic patterns (Fig. **2**, bottom panel). This precipitation pattern was successfully reproduced by a numerical simulation based on the sol-coagulation model (see section 2.2.3). Other investigations of $Ag_2Cr_2O_7$ precipitate patterns clearly demonstrated that the observed patterns satisfied the spacing and time

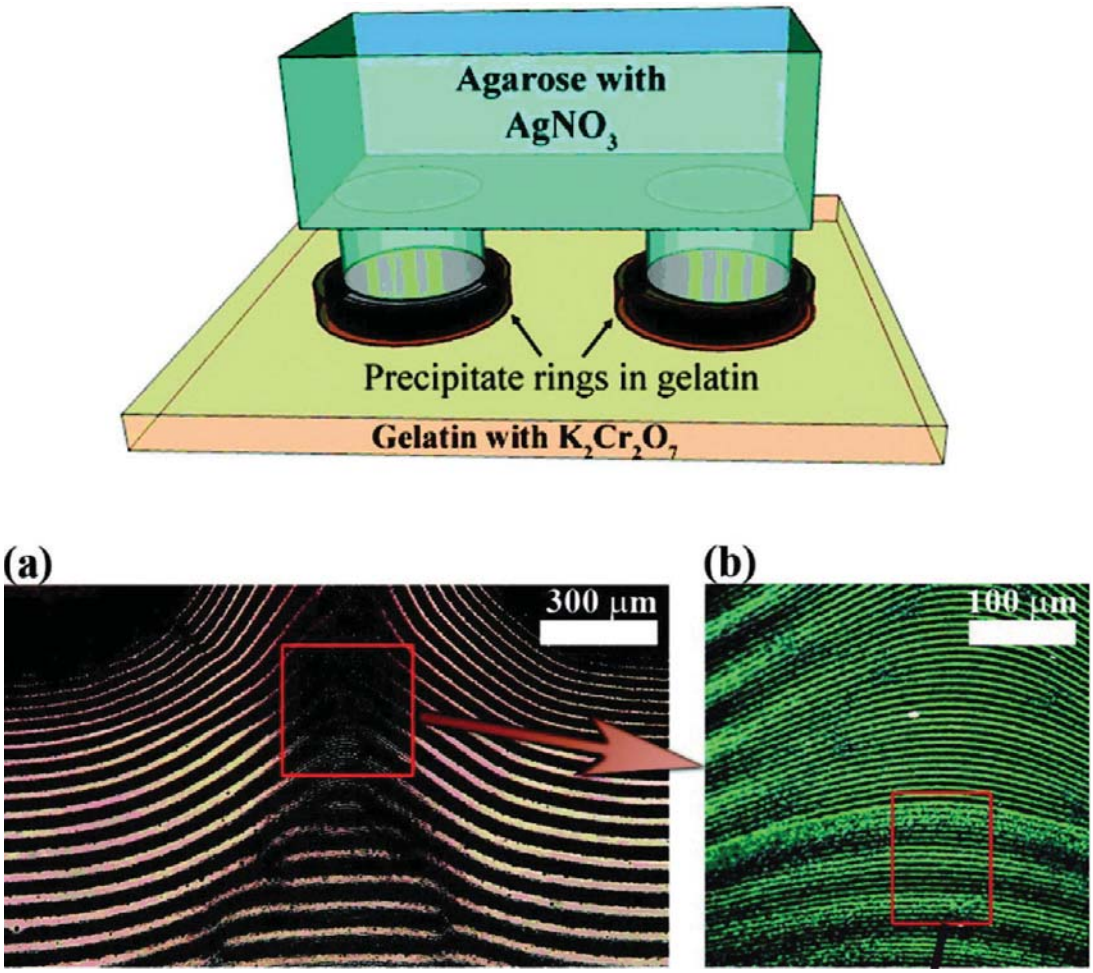

Fig. (2). (Top) Scheme of the experimental arrangement whereby the Liesegang patterns are propagated in $K_2Cr_2O_7$/gelatin film from circular features of an agarose stamp soaked with $AgNO_3$. (Bottom) Experimental images of the Liesegang patterns propagated from two nearby sources and featuring both primary and secondary bands. (**a**) A large-area optical image of the Liesegang patterns. The secondary bands are clearly visible in (**b**). Reprinted with permission from Ref. [23], Copyright 2011, American Chemical Society.

laws [24, 25]; $1 + p$ was evaluated to be 1.074-1.124, depending on the experimental conditions. A revert-type pattern, whose interband spacing decreases with increasing distance from the interface, has also been reported for AgI [36]. A comparison with numerical simulation results shows that the formation of AgI revert patterns is explained by assuming that the coagulation threshold varies in space and time because of the specific characteristics of AgI. Such examples of Ag-based precipitates have long been used as model experimental systems to gain mechanistic insights into Liesegang phenomena.

Recently, a unique Liesegang experiment was conducted in which the species doped in the gelation matrix was replaced by citric acid as a reducing agent for Ag^+ [59]. There is no ion pair that can spontaneously precipitate in this experimental configuration; therefore, the observation of Liesegang patterns consisting of a Ag-based material and formed by the conventional mechanism was not expected. However, very clear and unexpected Liesegang-like patterns formed within several hours (Fig. **3**). Qualitatively, the obtained patterns are similar to reported salt-based Liesegang patterns, *e.g.*, the interband spacing increases with increasing distance from the interface, which is indicative of satisfaction of the spacing law. Quantitative analysis suggests that the obtained ring patterns obey the spacing law (Fig. **4**), with $1 + p$ decreasing from 1.04 to 1.02 with increasing gelatin concentration. Such a gelatin-concentration-dependent decrease in $1 + p$ is a common feature of salt-based Liesegang patterns of Ag

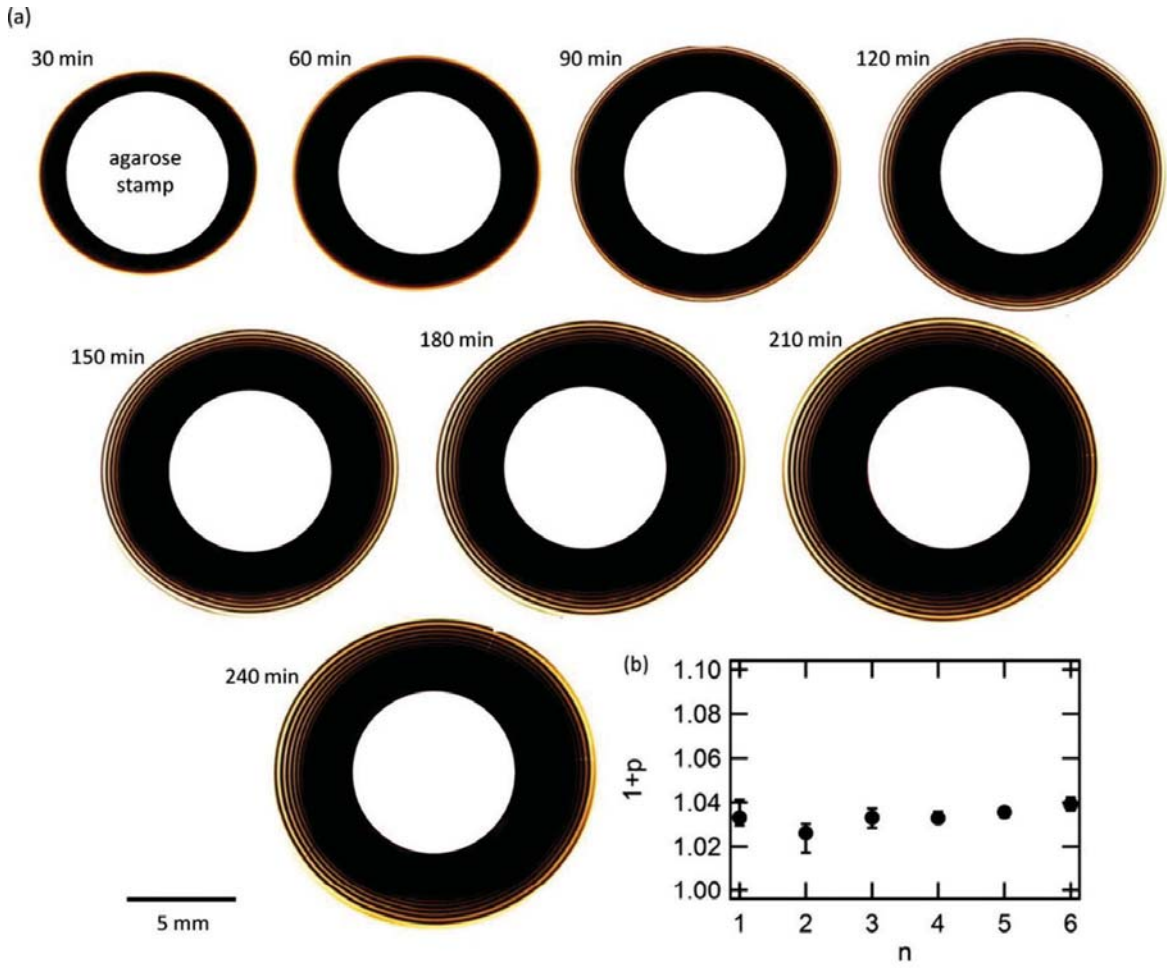

Fig. (3). (a) Optical microscope images of gelatin after contact with an agarose stamp. (b) Spacing-law plot for the rings in (**a**). The error bars in (**b**) indicate a standard deviation of $1 + p$ in each ring. Reprinted with permission from Ref. [59], Copyright 2014, American Chemical Society.

[25]. It can therefore be reasoned by analogy that the patterns that appear in the Ag^+/citric acid system are based on a Liesegang-like phenomenon.

Transmission electron microscopy showed that the ring region consisted of Ag nanoparticles with diameters of a few nanometers. The presence of Ag nanoparticles is also suggested by the bright plasmonic color of the observed rings (Fig. **3**). The reaction involved in this unusual system is not salt formation but reduction of Ag^+ ions by citric acid, which is a conventional chemical reaction for producing Ag nanoparticles. Such chemical reactions do not have concentration thresholds; therefore, this system clearly violates the criterion that requires a concentration threshold in the reaction, as described in section 2.2. Although the exact mechanism for the formation of Liesegang-like patterns in this system is still unclear, this study demonstrates the vast range of possible Liesegang phenomena. Unlike conventional Liesegang systems, which deposit salts, materials produced by chemical reactions other than salt-forming reactions are new materials for Liesegang patterning.

Another method for the formation of Liesegang patterns consisting of metal nanoparticles that is broadly based on a conventional Liesegang phenomenon has been reported [53]. In this system, the interdiffusing species are positively and negatively charged Au nanoparticles instead of the cations and anions in conventional systems. By controlling the surface charge and concentration of nanoparticles, Liesegang patterns consisting of metal nanoparticles were obtained (Fig. **5**). In this system, the reaction involved is salt formation between positively and negatively charged Au nanoparticles, in which the precipitation formation

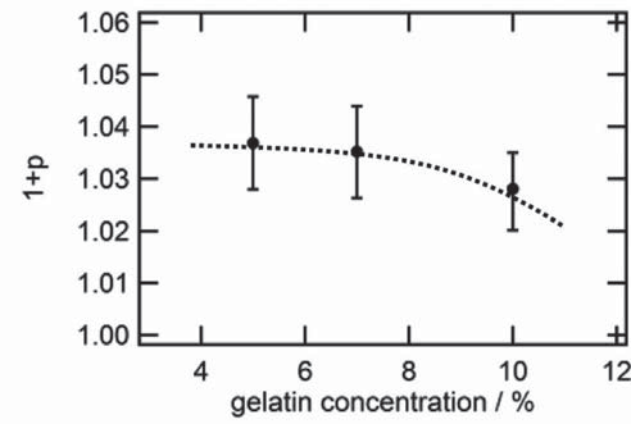

Fig. (4). Gelatin concentration dependence of p. Reprinted with permission from Ref. [59], Copyright 2014, American Chemical Society.

behavior is governed by the condition of charge neutrality. The formation of Liesegang patterns was therefore rationalized based on the nucleation and growth model by considering the concentration threshold derived from the nanoparticle charge neutrality condition. This method, which is essentially based on a conventional Liesegang phenomenon, enables the deposition of diverse materials.

Another example of a non-salt-based Liesegang system is the pattern formation by κ-carrageenan gel [60, 61]. Solution of κ-carrageenan are known to transform into gels by diffusion of gel-promoting ions; the gelation reaction has a concentration threshold, which is required to induce a conventional Liesegang mechanism. Diffusion of gel-promoting ions into a κ-carrageenan matrix results in gelation when the local ion concentration exceeds the threshold. Liesegang-like precipitation patterns that satisfy the spacing law are then formed. Although formation of this pattern occurs within the framework of a conventional Liesegang mechanism, it is unique because an ion-triggered reaction (with a concentration threshold) is used for the pattern formation.

These examples are important as they show that the exploration of novel reaction systems offers significant progress in the construction of Liesegang patterns with diverse materials. These systems provide clues for achieving precise control of the functionality of a patterned material.

3.2. Diversity in Pattern Geometry

In the previous section, we have seen that exploring novel reactions for Liesegang phenomena enables diverse materials to be deposited. In addition to material diversity, it is also important to control the pattern shape in order to develop sophisticated bottom-up self-assembly techniques. As the precipitation of Liesegang bands progresses one by one from the interface, precipitation is a good candidate method for constructing diverse complex structures. It is therefore highly important to control the precipitation process so that the shape of the Liesegang patterns is tuned in a controlled manner. One powerful approach for controlling the shape of the deposited patterns has been developed by Grzybowski's group; their technique is based on the use of microstamps with the desired geometry [62, 63]. As shown in Figs. (**3** & **5**), typical two-dimensional Liesegang experiments use a single circular gel stamp or liquid drop to acquire a defect-free single series of concentric ring patterns. In other words, changing the stamp shape could potentially yield Liesegang patterns with other geometries. This idea was realized using a wet stamping technique (WETS), in which an agarose stamp with a desired pattern shape containing an outer electrolyte is brought into contact with dry gelatin doped with an inner electrolyte. Diffusion of the outer electrolyte into the gelatin matrix induces the Liesegang phenomenon, and the pattern shape is determined by the stamp geometry.

Before discussing the geometric diversity of WETS-derived Liesegang patterns, we describe one important aspect of using microstamps as the source of the outer electrolyte instead of a liquid droplet, which becomes clear when we compare two similar systems [62]. Under normal Liesegang conditions, patterns are obtained by putting a liquid drop containing the outer electrolyte on a wet gelatin film doped with the inner electrolyte (Fig. **6a**, left). Intermixing of water between the liquid drop and wet gelatin disturbs formation of the fine pattern that would have appeared close to the interface. As a result, the first well-separated pattern appears 1 mm away from the interface. In contrast, under WETS conditions with an agarose stamp and dry gelatin (Fig. **6a**, right), water flow from the gelatin to the agarose is inhibited and

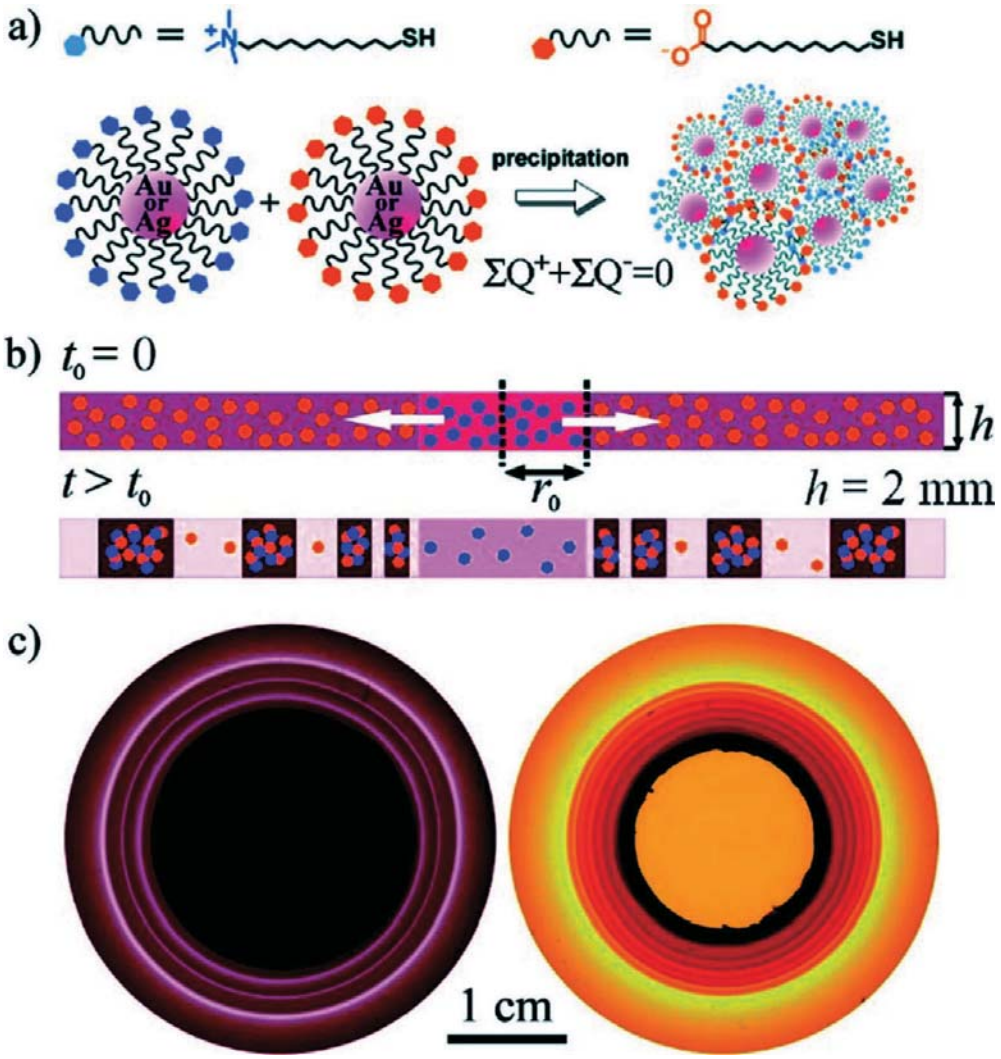

Fig. (5). Liesegang rings made of oppositely charged nanoparticles. (**a**) Structures of the charged alkane thiols $HS{-}(CH_2)_{11}{-}N(CH_3)^{3+}$ (TMA) and $HS{-}(CH_2)_{10}{-}COO^-$ (MUA) used to coat the nanoparticles. Irrespective of the properties of the metal cores, oppositely charged nanoparticles precipitate when their charges are balanced. (**b**) Cross-sectional view and typical dimensions of the gel layer supporting formation of nanoparticles-based Liesegang patterns. The rings appear after time $t \approx 24{-}36$ h. (**c**) Examples of ring structures formed by (left) 7.5 nm AuTMA (10.43 mM) nanoparticles delivered to a gel containing 7.4 nm AuMUA (2.26 mM) nanoparticles and (right) 9.7 nm AgTMA (9.47 mM) nanoparticles delivered into a gel soaked with 7.4 nm AgMUA (2.08 mM) nanoparticles. The characteristic hues of the patterns derive from the surface plasmon resonances (SPRs) of the particles (red-violet for Au nanoparticles and yellow-orange for Ag nanoparticles). Reprinted with permission from Ref. [53], Copyright 2010, American Chemical Society.

injection of the outer electrolyte into the gelatin is a diffusive process. This prevents fluidic disturbance and yields fine and well-separated patterns, even near the interface. These conditions enable miniaturization of Liesegang patterns from the centimeter and millimeter scales to the micrometer and nanometer scales.

As the WETS technique has the advantage of pattern formation close to the interface, it is possible to array several stamps close to each other. When a stamp with a square array of circular stamps is used, the outer electrolyte diffuses into the dry gelatin from each stamp (Fig. **6b**). The precipitation pattern appears from near the side of the interface of each stamp, resulting in the appearance of multiple concentric patterns. Furthermore, the patterns undergo interference between two adjacent stamps. As a result, the stamp array yields a characteristic pattern geometry that is not achievable using a single-stamp technique (Fig. **6c**). The geometry of these complex patterns can be controlled by the dimensions of the stamp,

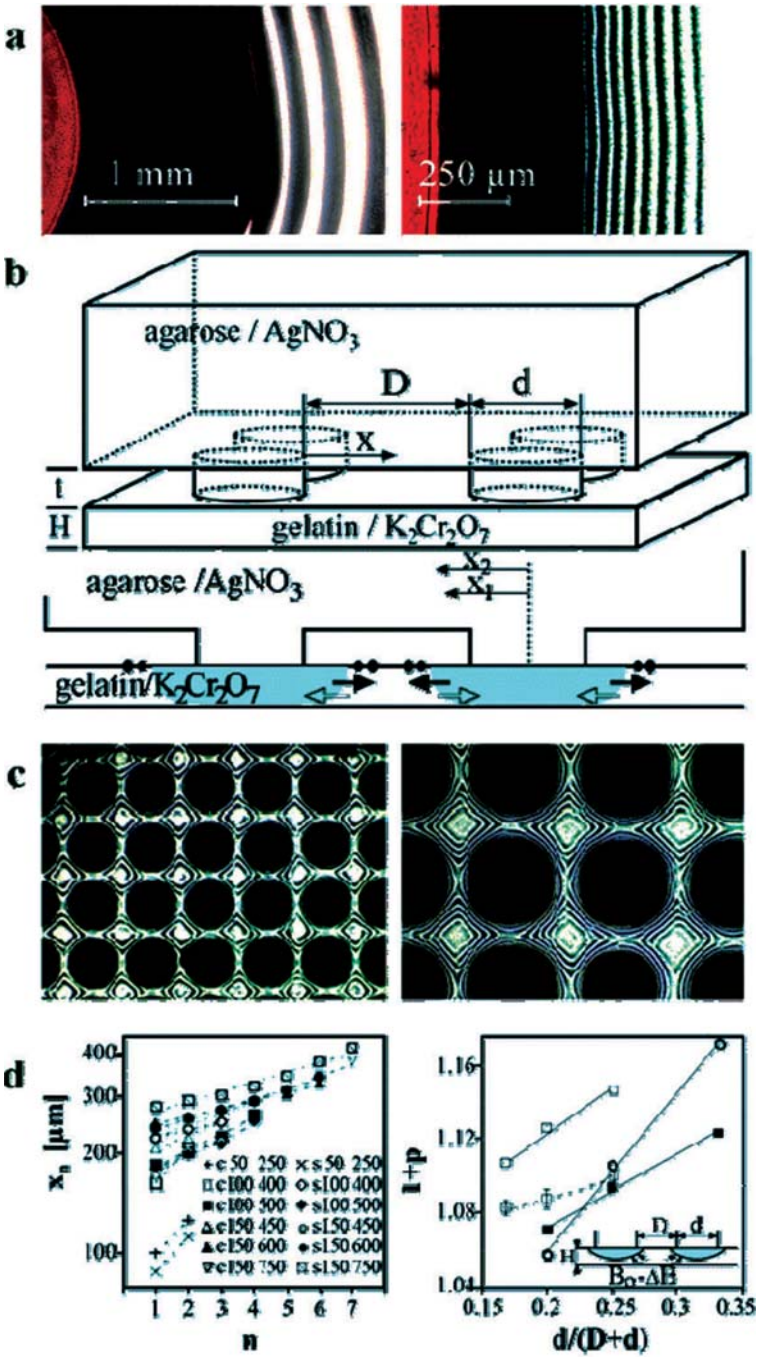

Fig. (6). (**a**) Liesegang patterns obtained from a macroscopic drop of 1 M $AgNO_3$ applied onto wet gelatin (left) and from an agarose block of similar dimensions placed on a dry gelatin layer (right); concentrations of inner and outer electrolytes were similar in both cases. (**b**) Scheme of the experimental arrangement and defined pertinent dimensions. The gray areas in the lower diagram correspond to transient precipitation zones. The arrows give approximate directions of diffusion of $AgNO_3$(solid arrows) and $K_2Cr_2O_7$(open arrows). Positions of Liesegang bands are indicated by solid ovals at the gelatin's surface. (**c**) Optical micrographs of regular Liesegang patterns obtained by stamping square arrays of circles (d = 100 μm, D = 300 μm, left picture) and squares (d = 150 μm, D = 600 μm, right picture). (**d**) The graph on the left gives the dependence of the radius of the nth ring x_n on the ring number in different square arrays of circles or squares. The notation in the legend specifies the shape of the stamped features (c, circles; s, squares), their dimensions (d, (μm), first column) and spacing (D, (μm), second column). The picture on the right shows the dependence of the spacing coefficient, $(1 + p)$, on the feature size-to-period ratio, $d/(D + d)$, for two square arrays of squares (d = 100 μm, open squares and d = 150 μm, open circles) and for a square array of circles (d = 150 μm, full circles). Markers on the dashed line are the results of numerical modeling of three square arrays of squares (d = 150 μm, D = 450, 600, 750 μm); each point is the average of 10 simulation runs, each starting with a different random seed for r. Reprinted with permission from Ref. [62], Copyright 2005, American Chemical Society.

such as the stamp diameter (d), interstamp distance (D), and stamp height (t). For example, by changing the shape of each stamp (circles and squares), the stamp diameter, and the interstamp distance, the radius of the nth pattern can be widely tuned (Fig. **6d**, left). Each condition maintains the linearity between the radius and the ring number n, which is a minimum requirement for a Liesegang phenomenon. The spacing coefficient can be controlled by the geometric parameters of the stamp, with the spacing coefficient linearly dependent on $d/(D + d)$ (Fig. **6d**, right). In addition to the stamp geometry, the thickness of the gelatin film (H) can be used as a parameter to control $1 + p$.

The WETS technique can be used to prepare multicolored micropatterns on thin dry gels [64]. Multicolored micropatterned materials are useful as non-binary optical elements and could form the basis of new applications in nano- and microscale systems. One example is the two-color patterns formed using an Fe/Cu coprecipitating system. In this experiment, a stamp with the desired pattern is codoped with Fe^{3+} and Cu^{2+} ions. The stamp is then placed on a gelatin film containing $[Fe(CN)_6]^{4-}$ ions, and the Fe^{3+} and Cu^{2+} ions diffuse into the gelatin film. The diffusivity of Cu^{2+} is larger than that of Fe^{3+}; therefore, the Cu^{2+} ions react with $[Fe(CN)_6]^{4-}$ first and form a layer of a Cu-based brown precipitate. The Fe^{3+} ions then diffuse through the region with the Cu-based precipitate and form a dark-blue Fe-based precipitate around the Cu-based precipitate zones. This system allows multicolor micropatterning with complex geometry to be achieved by changing the stamp geometry and ionic species.

3.3. Diversity in Regularity

As we have seen in section 2.1, Liesegang patterns have several regularities based on the spacing, time, and width laws. Regularity enables us to design a pattern construction with high spatiotemporal accuracy; therefore, to obtain well-ordered and tunable patterns, it is highly important to explore methods to control regularity. A simple approach for this purpose is the variation of experimental conditions such as the gel [17, 21, 25] and electrolyte concentrations [13, 44, 57, 60, 61]. However, a common feature of reaction-diffusion systems is that characteristic phenomena, such as wave or pattern formation, appear only under a narrow set of experimental conditions, which restricts the application and flexibility of these systems.

A powerful approach to expanding the tunability of pattern regularity is the use of an additional external bias. A typical example is electric fields, which have been applied to various systems such as $Co(OH)_2$ [8, 42, 43], $Mg(OH)_2$ [9], and $Ag_2Cr_2O_7$ [26, 29]. First, we assume a simple experimental setup, in which an open glass tube filled with $K_2Cr_2O_7$-doped gelatin is placed horizontally and in contact with $K_2Cr_2O_7$ and $AgNO_3$ solutions at each end [29]. Ag and Pt electrodes are immersed in the $AgNO_3$ and $K_2Cr_2O_7$ solutions, respectively, and these electrodes are connected to a power supply as the source of the electric field. Under conditions with and without the electric field, precipitation patterns of $Ag_2Cr_2O_7$ that satisfy the spacing law appear. The spacing coefficients vary from 1.041 to 1.144, depending on the direction and strength of the electric field. Furthermore, the electric field significantly changes the relationship between the position and time at which each band appears, *i.e.*, the time law. Without the electric field ($E = 0$ V m^{-1}), the location of the evolved Liesegang pattern is a linear function of the square root of time (Fig. **7**). This is a general rule, as we have seen in section 2.1(2). However, the presence of a non-zero electric field of any strength alters this linear relationship, which is now described by the function $x_n = a_1t^{1/2} + a_2t + a_3$. A numerical model based on the supersaturation model in the presence of an electric field can reproduce all the quantitative feature of these experiments. This non-linear time law in the presence of an external electric field was also observed when a vertical one-dimensional tube filled with gelatin containing $CoCl_2$ was used [43]. Concentrated ammonia was delivered to the top of the gelatin, and two electrodes were inserted into the ammonia (top of the tube) and $CoCl_2$ solutions (bottom of the tube) to control the vertical electric field strength.

The above-mentioned electric field dependence results from a direct current (DC) field. When an

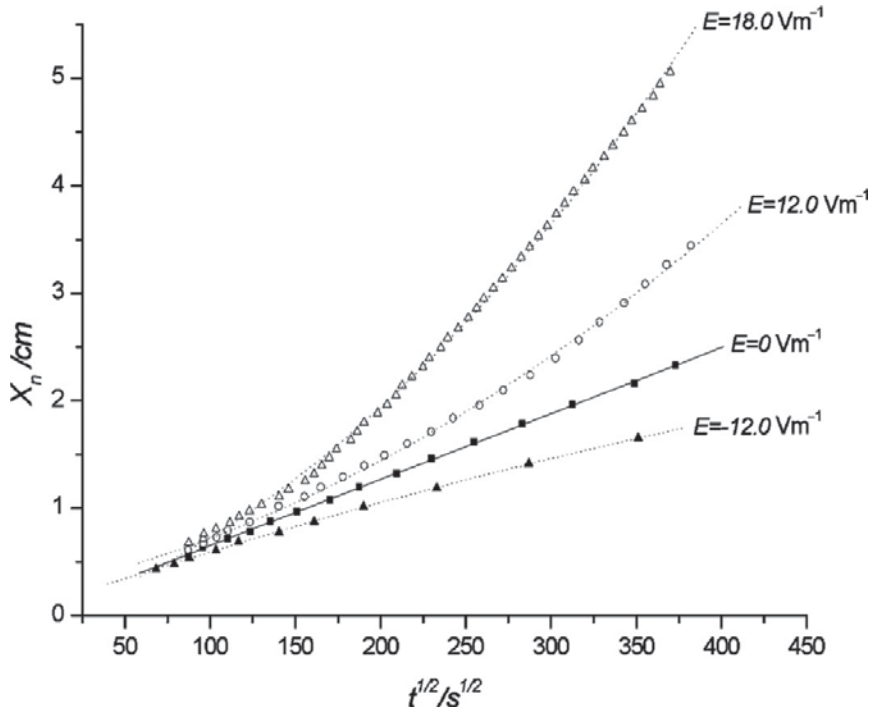

Fig. (7). Points show the distance of Liesegang rings, measured from the gel surface, as a function of the square root of formation time. The solid line represents the fitted linear curve for the electric-field-free case. The dotted lines represent the $x_n = a_1 t^{1/2} + a_2 t + a_3$ fitted curves for electric fields of various strengths. Reprinted with permission from Ref. [29], Copyright 2002, Royal Society of Chemistry.

alternating current (AC) field is used, the characteristics are completely different, as described below [8].

- The band spacing increases and reaches a plateau at large band numbers.
- The band spacing increases with increasing AC voltage, but to a lesser extent than with DC voltage under the same applied voltage.
- The band spacing increases with increasing frequency at low voltage.
- The band spacing becomes independent of the frequency at high voltage.
- The band spacing decreases with increasing inner electrolyte concentration, which is opposite to the behavior observed under a DC field.

The interaction between a reaction-diffusion system and electric fields under both AC and DC conditions can play an important role in controlling the regularity of pattern formation. In addition to the control obtained using chemical conditions, such as electrolyte concentration, physical parameters offer ways of controlling the periodicities of Liesegang patterns.

3.4. Diversity in Static/Dynamic Behavior

The various above-mentioned diversities have one common feature: the patterns formed are stationary and no dynamical change can be observed. This is a general feature of classical Liesegang phenomena and is a significant difference from dynamically changing spatial patterns such as the spiral wave of a BZ solution. However, a recent study has achieved BZ reaction-like dynamic behavior in Liesegang-like precipitation patterns, *i.e.*, a system that displayed characteristics of both static and dynamic pattern formation phenomena.

Typical dynamic pattern formation is reported using the precipitation and dissolution of $Al(OH)_3$ [65]. $AlCl_3$ is homogeneously dissolved as the inner electrolyte in agarose gel, and the outer electrolyte NaOH diffuses into the gel. Similar to classical Liesegang systems, nucleation and precipitation of $Al(OH)_3$ occurs; simultaneously, behind the nucleation and precipitation front, an

excess amount of OH^- reacts with $Al(OH)_3$ to form a complex (dissolution). These precipitation and complex formation processes shown in the following reactions resulted in the formation of a thin $Al(OH)_3$ precipitate band.

$$Al^{3+}(aq) + 3H_2O \quad Al(OH)_3(s) + 3H^+(aq)$$

$$Al(OH)_3(s) + H_2O \quad [Al(OH)_4]^-(aq) + H^+(aq)$$

As a result of the precipitation and dissolution propagation, the $Al(OH)_3$ precipitate band propagates with time, resulting in a dynamic Liesegang phenomenon.

It is reasonable to expect similar behavior to occur if a system can be designed to have both precipitation and dissolution processes. In fact, a recent study successfully realized dynamic precipitation patterns of $Zn(OH)_2$ and HgI_2, which are dissolvable as $[Zn(OH)_4]^{2-}$ and $[HgI_4]^{2-}$, respectively [66].

4. CONCLUSION

One of the fascinating features of Nature is the ability to self-organize complex spatiotemporal patterns. Many processes are involved, on levels ranging from intermolecular to intercellular reactions, in each self-organization system. Nature uses these interactions, with the aid of diffusion, to control the formation of diverse self-organized patterns. We can learn much from Nature on creating artificial self-organized patterns *via* similar strategies. The reaction-diffusion dynamics seen in Nature can be easily reproduced in petri dishes or glass tubes. The next step we have to take is to further link the reaction-diffusion phenomena in Nature with chemical model systems. Such successful linkages will give us deep mechanistic insights into how Nature uses and harmonizes reactions among constituents. These reaction networks will in turn provide good methods for producing artificial mimicking systems. Continuous repetition of this process of linking, understanding, and mimicking is the only way for us to approach the complexity seen in Nature. The Liesegang phenomenon is a typical example, and throughout its long history, it has stimulated diverse research interests in many other fields in addition to chemistry. Developments in Liesegang research in fields such as chemistry, engineering, biology, physics, and petrology enable comprehensive understanding of Liesegang reactions in Nature. Furthermore, such comprehensive knowledge provides ways of controlling the reaction-diffusion mechanism involved in the Liesegang phenomenon, enabling the construction of complex artificial Liesegang patterns, which will lead to as yet unsuspected novel research areas.

CONFLICT OF INTEREST

The author confirms that this article content has no conflict of interest.

ACKNOWLEDGEMENTS

Declared none.

REFERENCES

[1] Gilchrist, H.M.; Wick, M.R.; Patterson, J.W. Liesegang rings in an apocrine hidrocystoma: A case report and review of literature. *J. Cutaneous Pathol.*, **2010**, *37*, 1064-1066.

[2] Khonsari, R.H.; Calvez, V. The origins of concentric demyelination: Self-organization in the human brain. *PLoS One*, **2007**, *1*, e150.

[3] Kondo, S.; Asai, R. A reaction-diffusion wave on the skin of the marine angelfish Pomacanthus. *Nature*, **2002**, *376*, 765-768.

[4] Müller, S.C.; Kai, S.; Ross, J. Curiosities in periodic precipitation patterns. *Science*, **1982**, *216*(4546), 635-637.

[5] Müller, S.C.; Kai, S.; Ross, J. Periodic precipitation patterns in the presence of concentration gradients. 1. Dependence on ion product and concentration difference. *J. Phys. Chem.*, **1982**, *86*(20), 4078-4087.

[6] Kai, S.; Müller, S.C.; Ross, J. Periodic precipitation patterns in the presence of concentration gradients. 1. Spatial bifurcation of precipitation bands and stochastic pattern formation. *J. Phys. Chem.*, **1983**, *87*(5), 806-813.

[7] Tinsley, M.R.; Collison, D.; Showalter, K. Propagating precipitation waves: experiments and modeling. *J. Phys. Chem. A*, **2013**, *117*(48), 12719-12725.

[8] Karam, T.; Sultan, R. Effect of an alternating current electric field on $Co(OH)_2$ periodic precipitation. *Chem. Phys.*, **2013**, *412*, 7-12.

[9] Al-Ghoul, M.; Ammer, M.; Al-Kaysi, R.O. Band propagation, scaling laws and phase transition in a precipitate system. I: Experimental study. *J. Phys. Chem. A.*, **2012**, *116*(18), 4427-4437.

[10] Molnár, F.; Roszol, L.; Volford, A.; Lagzi, I. Control of precipitation pattern in two-dimensions by pH field. *Chem. Phys. Lett.*, **2011**, *503*, 231-234.

[11] Badr, L.; Moussa, Z.; Hariri, A.; Sultan, R. Band, target, and onion patterns in $Co(OH)_2$ Liesegang systems. *Phys. Rev. E*, **2011**, *83*, 016109/1-016109/6.

[12] Voford, A.; Lagzi, I.; Molnár, F.; Rácz, Z. Coarsening of precipitation patterns in a moving reaction-diffusion front. *Phys. Rev. E*, **2009**, *80*, 055102/1-055102/4.

[13] Badr, L.; Sultan, R. Ring morphology and pH effects in 2D and 1D $Co(OH)_2$ Liesegang systems. *J. Phys. Chem. A*, **2009**, *113*(24), 6581-6586.

[14] Batlouni, H.; Al-Ghoul, M. Experimental study of the dynamics of front propagation in the $Co(OH)_2/NH_4OH$ Liesegang system using spectrophotometry. *J. Phys. Chem. A*, **2008**, *112*(35), 8038-8045.

[15] El-Batlouni, H.; El-Rassy, H.; Al-Ghoul, M. Cosynthesis, coexistence and self-organization of α- and β-cobalt hydroxide based on diffusion and reaction in organic gels. *J. Phys. Chem. A*, **2008**, *112*(34), 7755-7757.

[16] Msharrafieh, M.; Al-Ghoul, M.; Batlouni, H.; Saltan, R. Front propagation in patterned precipitation. 3. Composition variations in two-precipitate stratum dynamics. *J. Phys. Chem. A*, **2007**, *111*(30), 6967-6976.

[17] Thomas, S.; Varghese, G.; Bárdfalvy, D.; Lagzi, I.; Rácz, Z. Helicoidal precipitation patterns in silica and agarose gels. *Chem. Phys. Lett*., **2014**, *599*, 159-162.

[18] Kalash, L.; Farah, H.; Eddin, A.Z.; Sultan, R. Dynamical profile of the reactive components in direct and revert Liesegang patterns. *Chem. Phys. Lett.*, **2013**, *590*, 69-73.

[19] Thomas, S.; Lagzi, I.; Molnár, F.; Rácz, Z. Helices in the wake of precipitation fronts. *Phys. Rev. E*, **2013**, *88*, 022141/1-022141/6.

[20] Thomas, S.; Lagzi, I.; Molnár, F.; Rácz, Z. Probability of the emergence of helical precipitation patterns in the wake of reaction-diffusion fronts. *Phys. Rev. Lett.*, **2013**, *110*, 078303/1-078303/5.

[21] Lagzi, I. Controlling and engineering precipitation patterns. *Langmuir*, **2012**, *28*(7), 3350-3354.

[22] Karam, T.; El-Rassy, H.; Sultan, R. Mechanism of revert spacing in a $PbCrO_4$ Liesegang system. *J. Phys. Chem. A*, **2011**, *115*(14), 2994-2998.

[23] Smoukov, S.K.; Lagzi, I.; Grzybowski, B.A. Independent of primary and secondary structures in periodic precipitation patterns. *J. Phys. Chem. Lett.*, **2011**, *2*(4), 345-349.

[24] Pan, C.; Gao, Q.; Xie, J.; Xia, Y.; Epstein, I.R. Precipitation patterns with polygonal boundaries between electrolytes. *Phys. Chem. Chem. Phys.*, **2009**, *11*, 11033-11039.

[25] Lagzi, I.; Ueyama, D. Pattern transition between periodic Liesegang pattern and crystal growth regime in reaction-diffusion systems. *Chem. Phys. Lett.*, **2009**, *468*(4-6), 188-192.

[26] Bena, I.; Droz, M.; Lagzi, I.; Martens, K.; Rácz, Z.; Volford, A. Designed patterns: Flexible control of precipitation through electric currents. *Phys. Rev. Lett.*, **2008**, *101*, 075701/1-075701/4.

[27] Fialkowski, M.; Bitner, A.; Grzybowski, B.A. Wave optics of Liesegang rings. *Phys. Rev. Lett.*, **2005**, *94*, 018303/1-018303/3.

[28] Lagzi, I.; Volford, A.; Büki, A. Effect of geometry on the time law of Liesegang patterning. *Chem. Phys. Lett.*, **2004**, *396*, 97-100.

[29] Lagzi, I. Formation of Liesegang patterns in an electric field. *Phys. Chem. Chem. Phys*., **2002**, *4*, 1268-1270.

[30] Karam, T.; El-Rassy, H.; Zaknoun, F.; Moussa, Z.; Sultan, R. Lisegang bandind and multiple precipitate formation in cobalt phosphate systems. *Chem. Phys. Lett.*, **2012**, *525-526*, 54-59.

[31] Suetsugu, Y.; Walsh, D.; Tanaka, J.; Mann, S. Hydroxyapatite pattern formation in PVA gels. *J. Mater. Sci.*, **2009**, *44*(21), 5806-5814.

[32] Parekh, B.; Joshi, M.; Vaidya, A. Characterization and inhibitive study of gel-grown hydroxyapatite crystals at physiological temperature. *J. Cryst. Growth*, **2008**, *310*(7-9), 174-1753.

[33] George, J.; Varghese, G. Intermediate colloidal formation and the varying width of periodic precipitation bands in reaction-diffusion systems. *J. Colloid Interface Sci.*, **2005**, *282*(2), 397-402.

[34] Makki, R.; Al-Ghoul, M.; Sultan, R. Propagating fronts in this tubes: Concentration, electric, and pH effects in a two-dimensional precipitation pulse system. *J. Phys. Chem. A*, **2009**, *113*(21), 6049-6057.

[35] Ayass, M.M.; Al-Ghoul, M. Superdiffusive cusp-like waves in the mercuric iodide precipitate system and their transition to regular reaction bands. *J. Phys. Chem. A*, **2014**, *118*(22), 3857-3865.

[36] Molnár, F.; Izsák, F.; Lagzi, I. Design of equidistant and revert type precipitation patterns in reaction-diffusion systems. *Phys. Chem. Chem. Phys.*, **2008**, *10*, 2368-2373.

[37] Ripszám, M.; Nagy, Á.; Volford, A.; Izsák, F.; Lagzi, I. The Liesegang eyes phenomenon. *Chem. Phys. Lett.*, **2005**, *414*, 384-388.

[38] Toramaru, A.; Harada, T.; Okamura, T. Experimental pattern transitions in a Liesegang system. *Phyica D*, **2003**, *183*(1-2), 133-140.

[39] Ayass, M.M.; Mansour, A.A.; Al-Ghoul, M. Alternating metastable/stable pattern in the mercuric iodide crystal formation outside the Ostwald rule of stages. *J. Phys. Chem. A*, **2014**, *118*(36), 7725-7731.

[40] Xie, A.J.; Zhang, L.; Zhu, J.; Shen, Y.H.; Xu, Z.; Zhu, J.M.; Li, C.H.; Chen, L.; Yang, L.B. Formation of calcium oxalate concentric precipitate rings in two-dimensional agar gel systems containing Ca^{2+} - RE^{3+} (RE = Er, Gd, and La) - $C_2O_4^{2-}$. *Colloids and Surfaces A*, **2009**, *332*(2-3), 192-199.

[41] Maddalian, L.; Fahs, M.; Al-Ghoul, M.; Sultan, R. Morphology, particle size distribution, and composition in one- and two-salt metal oxinate Liesegang patterns. *J. Phys. Chem. B*, **2004**, *108*(4), 1507-1514.

[42] Shreif, Z.; Mandalian, L.; Abi-Haydar, A.; Sultan, R. Taming ring morphology in 2D $Co(OH)_2$ Liesegang patterns. *Phys. Chem. Chem. Phys.*, **2004**, *6*, 3461-3466.

[43] Sultan, R.; Halabieh, R. Effect of an electric field on propagating $Co(OH)_2$ Liesegang patterns. *Chem. Phys. Lett.*, **2000**, *332*, 331-338.

[44] Rajurkar, N.; Ambekar, B. Studies on Liesegang rings of copper molybdate in agar gel medium. *J. Mol. Liquids*, **2013**, *180*, 70-73.

[45] Wagner, C. Mathematical analysis of the formation of periodic precipitations. *J. Colloid Sci.*, **1950**, *5*(1), 85-97.

[46] Prager, S. Periodic precipitation. *J. Chem. Phys.*, **1956**, *25*(2), 279-283.

[47] Keller, J.B.; Rubinow, S.I. Recurrent precipitation and Liesegang rings. *J. Chem. Phys.*, **1981**, *74*(9), 5000-5007.

[48] Feeney, R.; Schmidt, S.L.; Strickholm, P.; Chandam, J.; Ortoleva, P. Periodic precipitation and coarsening waves: Applications of the competitive particle growth model. *J. Chem. Phys.*, **1983**, *78*(3), 1293-1311.

[49] Venzl, G. Pattern formation in precipitation processes. I. The theory of competitive coarsening. *J. Chem. Phys.*, **1986**, *85*(4), 1996-2005.

[50] Venzl, G. Pattern formation in precipitation processes. II. A Postnucleation theory of Liesegang bands. *J. Chem. Phys.*, **1986**, *85*(4), 2006-2011.

[51] Rácz, Z. Formation of Liesegang patterns. *Physica A.*, **1999**, *274*(1-2), 50-59.

[52] Ostwald, W. Lehrbuch der allgemeinen Chemie, Z. *Anorganische Chemie*, **1897**, *15*(1), 239.

[53] Lagzi, I.; Kowalczyk, B.; Grzybowski, B.A. Liesegang rings engineered from charged nanoparticles. *J. Am. Chem. Soc.*, **2010**, *132*(1), 58-60.

[54] Dhar, N.R.; Chatterji, A.C. Studies on the formation of periodic precipitates. II. *J. Phys. Chem.*, **1924**, *28*(1), 41-50.

[55] Shinohara, S. A theory of one-dimensional Liesegang phenomena. *J. Phys. Soc. Jpn.*, **1970**, *29*(4), 1073-1087

[56] Antal, T.; Droz, M.; Magnin, J.; Rácz, Z. Formation of Liesegang patterns: A spinodal decomposition scenario. *Phys. Rev. Lett.*, **1999**, *83*(15), 2880-2883.

[57] Thomas, S.; Molnar, F.; Rácz, Z.; Lagzi, I. Matalon-Packter law for stretched helicoids formed in precipitation processes. *Chem. Phys. Lett.*, **2013**, *577*, 38-41.

[58] Lagzi, I.; Papai, P.; Rácz, Z. Complex motion of precipitation bands. *Chem. Phys. Lett.*, **2007**, *433*, 286-291.

[59] Nabika, H.; Sato, M.; Unoura, K. Liesegang patterns engineered by a chemical reaction assisted by complex formation. *Langmuir*, **2014**, *30*(18), 5047-5051.

[60] Narita, T.; Ohnishi, I.; Tokita, M.; Oishi, Y. Macroscopic pattern formation of liquid crystal in κ-carrageenan gel. *Colloids Surfaces A*, **2008**, *321*(1-3), 117-120.

[61] Narita, T.; Tokita, M. Liesegang pattern formation in κ-carrageenan gel. *Langmuir*, **2006**, *22*(1), 349-352.

[62] Bensemann, I.T.; Fialkowski, M.; Grzybowski, B.A. Wet stamping of microscale periodic precipitation patterns. *J. Phys. Chem. B*, **2005**, *109*(7), 2774-2778.

[63] Campbell, C.J.; Klajn, R.; Fialkowski, M.; Grzybowski, B.A. One-step multilevel microfabrication by reaction-diffusion. *Langmuir*, **2005**, *21*(1), 418-423.

[64] Klajn, R.; Fialkowski, M.; Bensemann, I.T.; Bitner, A.; Campbell, C.J.; Bishop, K.; Smoukov, S.; Grzybowski, B.A. Multicolour micropatterning of thin films of dry gels. *Nat. Mater.*, **2004**, *3*, 729-735.

[65] Volford, A.; Izsák, F.; Ripszám, M.; Lagzi, I. Pattern formation and self-organization in a simple precipitation system. *Langmuir*, **2007**, *23*(3), 961-964.

[66] Ayass, M.M.; Al-Ghoul, M.; Lagzi, I. Chemical waves in heterogeneous media. *J. Phys. Chem. A*, **2014**, *118*, 11678-11682.

Received: November 12, 2014 **Revised: December 25, 2014** **Accepted: March 15, 2015**